〈報文〉 HWAHAK KONGHAK Vol. 17, No. 2, April 1979, pp. 109—116
(Journal of the Korean Institute of Chemical Engineers)

기체 유동상 내에서 고체 입자 혼합에 미치는 온도의 영향

金 海 植 · 李 源 國

韓國科學院 化學工學科

(接受 1979. 3. 3)

Temperature Effect on Solid Mixing in a Gas-Fluidized Bed

Hai-Sik Kim and Won Kook Lee

Department of Chemical Engineering
Korea Advanced Institute of Science, Seoul 132, Korea

(Received March 3, 1979)

요 약

유동층상에서 유동입자의 혼합효과에 대한 온도의 영향을 체류시간 분포(RTD)를 측정하여 정량적으로 연구하였다. 변수로서 온도와 함께 기체유속, aspect ratio (bed의 직경에 대한 높이의 비)를 고려하였다. 실험의 결과 온도의 상승에 따른 u_{mf} 추정식에 의한 예상보다 실제 빨리 fluidization 되기 시작했다. 기체의 유속과 aspect ratio가 유동입자의 혼합효과에 커다란 영향을 미쳤으나 온도의 영향은 작게 나타났다.

Abstract

The effect of temperature on solids mixing rate was investigated quantitatively by measuring the residence time distribution (RTD) in a co-current gas-solid fluidized bed. The variables selected for this investigation were temperature, gas flow rate and aspect ratio which is ratio of the bed height to diameter. The experimental results showed that the onset of fluidization occurred earlier than the expected velocity as the temperature rise. The results also showed that the gas flow rate and aspect ratio had a marked effect on the mixing pattern of solids, but temperature elevation increased the mixing effect slightly.

I. Introduction

Because the effects of solids mixing on heat transfer, mass transfer and chemical conversion in a gas-fluidized bed are important, many have been investigating on the solids mixing. There have been two main lines attacking on the problem of solids mixing, one of which makes use of a concept of residence time distribution and the other is the concept of axial diffusion. Reported experimental findings [1),2)] show that the bubble phase is the chief contributor to the process of mixing and that the solids mixing rate is affected mainly by the flow rate of fluidizing fluid, the physical properties of solid and the physical properties of fluidizing fluid. Numerous studies have been made on the measurement of the basic physical properties of fluidized systems. [7)~10)] In particular, in recent years much research has been done into the study of solids mixing in a fluidized bed. Fluidized processes are mainly conducted at high temperature. However, almost all researches on solids mixing in fluidized beds has been done at room temperature.

In the present work, therefore, an attempt was made to investigate the temperature effect on solids mixing together with fluid flow rate and aspect ratio. The experiments were carried out with glass powder, and colored glass powder as a tracer material in a co-current gas-solid fluidized bed at a steady state with continuous feed and discharge of solids.

II. Theoretical Background

The perfect mixing deviation models are suggested as follows;

Perfect mixing with plug flow
Perfect mixing with dead space
Perfect mixing with partial short circuiting
Perfect mixing with error in average residence time
Perfect mixing with lag in response

The most general case is obtained by combining all the preceding models to determine the equation for the resulting F-function.

Wolf and Resnick[6)] developed the residence time distribution for real system by a F-function of the form

$$F(t)=1-\exp\left[-\eta\frac{t-\alpha}{\theta}\right] \quad \text{for } t\geq\alpha$$

$$F(t)=0 \quad \text{for } t<\alpha$$

The term η can be said to be a measure of the efficiency of mixing and the term α is a measure of the phase shift in the system. In *Table* 1, the values for η and α/θ are shown for various models.

The value η and α/θ can be calculated by slope and intercept from the log-log plot of $F(t)$ against t/θ. The dependency and degree of mixing in various conditions are found from the plot, and it plays a role to predict the operating conditions.

For the case of perfect mixing, η is equal to unity, whereas for pure plug flow, η tends to infinity. Therefore, it can be said that $(\eta-1)$ represents the degree of the perfect mixing deviation.

Table 1. Values of η and α/θ

Model	η	α/θ
perfect mixing	1	0
with plug flow	>1	>0
with dead space	>1	0
with short circuiting	<1	<0
with error in	≷1	0
with system lag	1	>0

Ⅲ. Experiment

1. Apparatus and Material

A schematic diagram of the experimental equipments is given in *Fig.* 1. The fluidizing air was supplied by a 1 h.p. air compressor through a pressure regulator, and the flow rate of air was measured with a rotameter which was calibrated by using a wet-test meter. The air was led to pass through the $CaCl_2$ dehumidifier and through the heating system which is controlled by on-off temperature controller, and then to the fluidized bed.

A sintered disc was used as the air distributor. The fluidized bed was of stainless steel, 7.8 cm diameter and 150 cm high. Solids were added to the top of the bed through 1 cm diameter tube with a screw feeder. A voltage regulator in the feeder regulated the feed rate of solids.

Pressure drops of the bed were measured by a H_2O manometer, and the fine particles in the effluent gas stream were recovered by two cyclons. A 1 cm diameter downcomer was used for discharging the solids and contolling the depth of the bed.

The heating system was made of a glass tube, 10 cm diameter and 600 cm total length, and electrical resistance heating coil within the tube. Glass beads were used for the fluidizing solid particles, and the physical properties were listed in *Table* 2. Blue colored glass beads were used as the tracer, and which was almost identical property with the white material.

Table 2. Experimental Materials

Particle	white glass bead
Tracer	blue glass bead
	$\bar{d}_p=0.175$ cm
	$\rho_s=2.45$ g/cm^3
	$\phi=0.6$
	$\epsilon_{mf}=0.5825$
Fluidizing gas	air

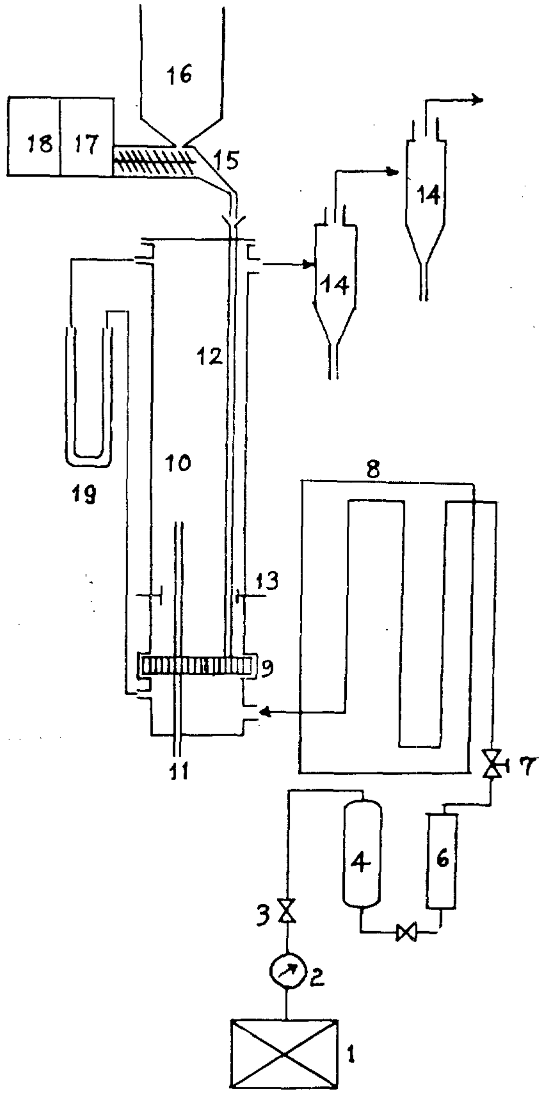

1. compressor
2. pressur regulatore
4. dehumidifier
3, 5. needle valve
6. rotameter
7. plug cock
8. heating system
9. gas distributor
10. fluidized bed
11. overflow pipe
12. feeding pipe
13. thermocouple
14. cyclon
15. screw feeder
16. hopper
17. D.C. motor
18. volt regulator
19. manometer

Fig. 1 Schematic Diagram of Experimental Apparatus

2. Procedure

Minimum fluidization velocities of glass powder at various temperatures were examined by measuring the pressure drops.

Experiments were carried out by initially charging the bed with the tracer material which was weighed according to the aspect ratio (L/D). Pressure regulated air ($2\,kg/cm^2$ gauge) was introduced in the bed through the heating system, and the gas flow rate was controlled and checked by a valve and a rotameter, respectively. After fluidizing a few minute with no detectable variation in temperature throughout the bed, the over flow pipe (down-comer) was set on the expansion bed height. White glass powder was then fed in, and solids were removed from the over flow pipe such that the feed rate equalled the rate of removal. Samples were taken at the outlet at specified time intervals.

After the operation, the screw feeder was off and the gas valve was closed immediately. The feeding time was checked. The contents in the bed and residue of the glass powder in the feeder were drawn out and weighed. With the empty bed, the above procedure was repeated for another run.

Experimental conditions are tabulated in *Table* 3.

Table 3. Experimental Conditions

Aspect ratio	variable	$L/D=1, 2, 3$
Particle size	constant	$d_p=60-120$ mesh
Gas velocity	variable	$u_0/u_{mf}=1.5, 2.0, 2.5$
Solids feed rate	constant	$v=0.88$ g/sec
Temperature	variable	$T=20, 80, 140, 200°C$

3. Analytical Equipment

Analysis of samples of the solids was conducted by measuring the intensity of the reflected beam with a cadmium sulfide photoconductive cell. Since the cell was insensitive to blue light, the intensity of the reflected beam decreased with increase in the concentration of blue particles in the sample, and the out of balance current calibrated against the concentration of blue particles. Use of this method enabled rapid analysis of samples of glass powder.[5]

The analytical equipment is shown in *Fig.* 2, which also shows the circuit diagram. The photoconductive cell gave rise to out-of-balance currents measurable without amplication on a galvanometer. The galvanometer was calibrated by using samples of known composition.

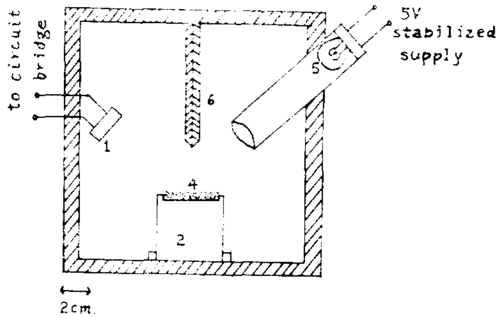

1. CdS photocell
2. sample cell
3. guides
4. sample
5. bulb
6. baffle

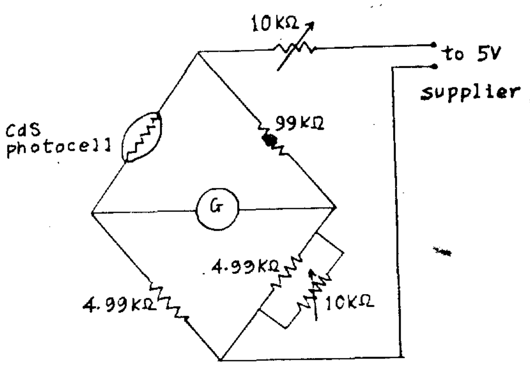

Fig. 2. Analytical Equipment and Circuit Bridge

Ⅳ. Results and Discussions

1. Minimum Fluidization Velocity with Temperature Changes.

Fig. 3 shows the experimental pressure-drop-flow diagrams of the bed across the distributor. If the air flow rate is first increased and then decreased, two slightly different pressure-drop-flow diagrams were obtained due to variations in the voidage of the packed bed. The plots show two well defined straight-line regions with slight irregularities near the point of incipient fluidization, probably due to channelling.[4]

The minimum fluidizing velocity u_{mf} is given theoretically as[3]

$$u_{mf}=\frac{(\phi d_p)^2}{150}\ \frac{\rho_s-\rho_g}{\mu}g\ \frac{\epsilon_{mf}}{1-\epsilon_{mf}}$$

$$Re_p<20 \qquad (3)$$

Substituting the values given in *Table* 2 and $\mu=1.899\times10^{-4}$ poise (air) at 20°C into Eq(3),

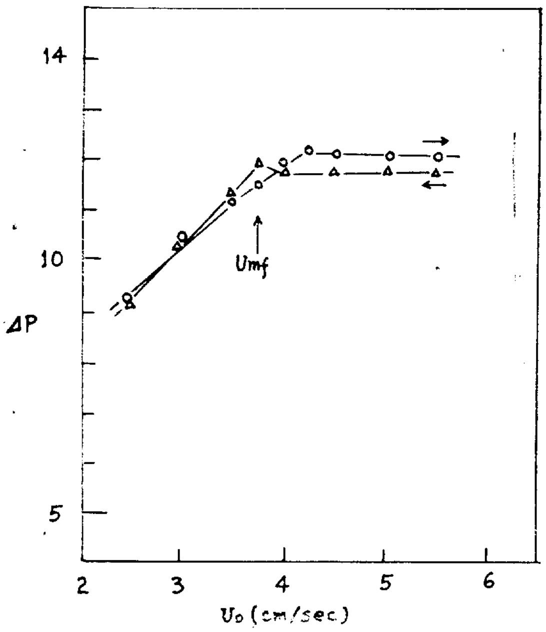

Fig. 3. Pressure-Drop Flow Diagram

u_{mf} is obtained as 4.446. Similarly, it can be calculated u_{mf} by changing the value of μ at each temperature. *Fig.* 4 shows the measured u_{mf} in the range from 20°C to 200°C, and compared these with calculated values.

It indicates that the onset of fluidization occures earlier than the expected velocity as the temperature rise.

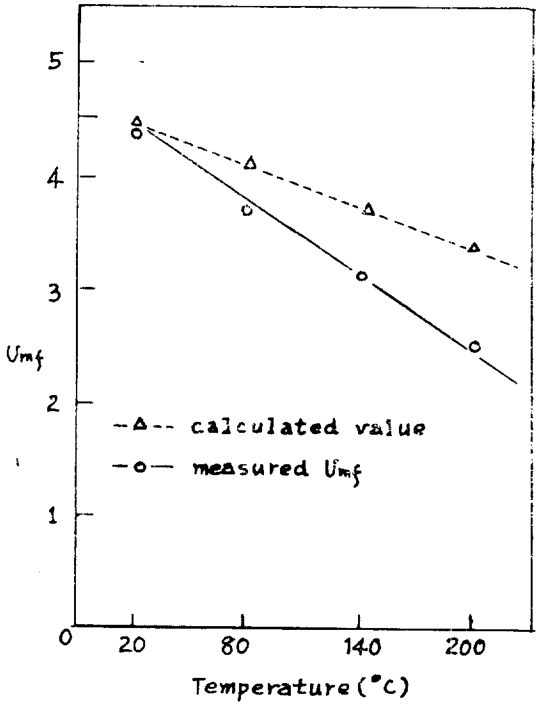

Fig. 4. Theoretical and Experimental u_{mf}

2. Mixing Efficiency and Correlation

The F-diagram with step input was obtained by plotting the percent concentration of sample material against the quantity t/θ. The typical F-diagram is shown in *Fig.* 5. From this F-diagram, η and α can be obtained.

The relationship between η and the system variables proposed by the authors is as follows:

$$(\eta-1)=k(u_0/u_{mf})^a(L/D)^b(T/T_0)^c \qquad (4)$$

Where k is the coefficient; a, b and c are the respective exponents of the system variables.

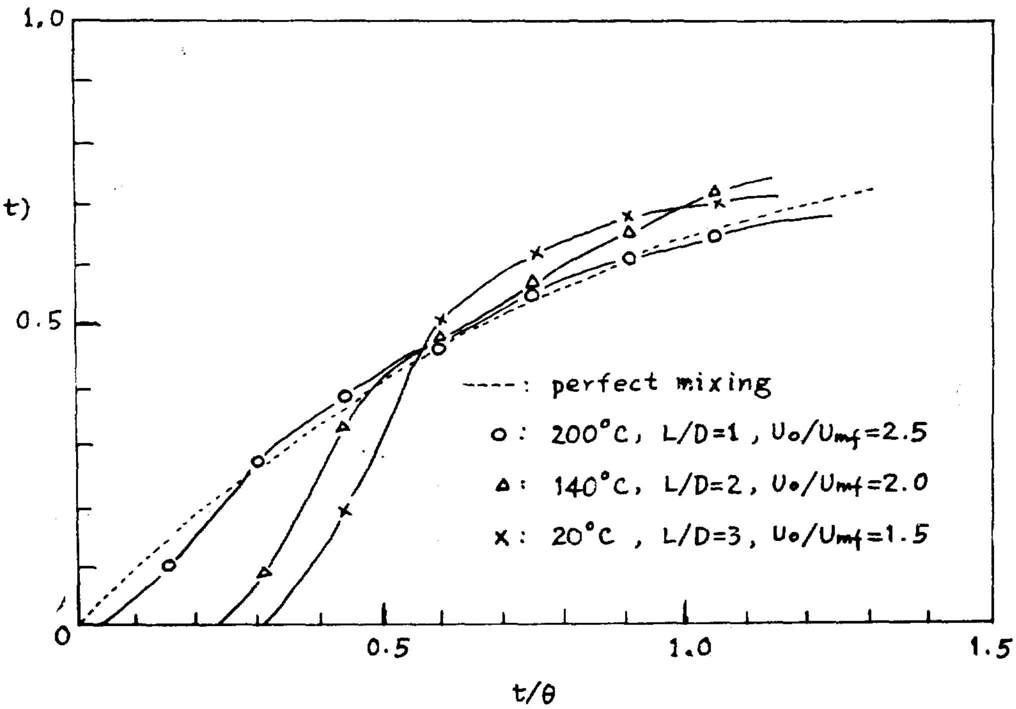

Fig. 5. Typical *F*-Diagram

T_0 is the temperature at 20°C. To get the constant and exponents of Eq(4), the effects of variables on η were observed.

Effect of fluid velocity······ η is found to be strong function of fluid velocity. This is obvious, because increased gas velocity results in increase in the number of rising gas bubbles, which favour random shuffling of the particles, leading to a better dispersed homogeneous mass of materials. The average slope form *Fig.* 6 for the exponent a was −1.411.

Effect of aspect ratio ······Since the bed diameter was not varied, increase in the bed height, *L*, implies that the amplitude of movement of the mobile particles within the bed is partly arrested or hindered and there is a tendency of segregation, resulting in poor mixing. So the value $(\eta-1)$ was increased with increasing of L/D and the exponent of *b* was 0.897 in *Fig.* 7.

Effect of temperature······ For the frequency fo bubble formation tends to increase with temperature, the mixing efficiency is increased

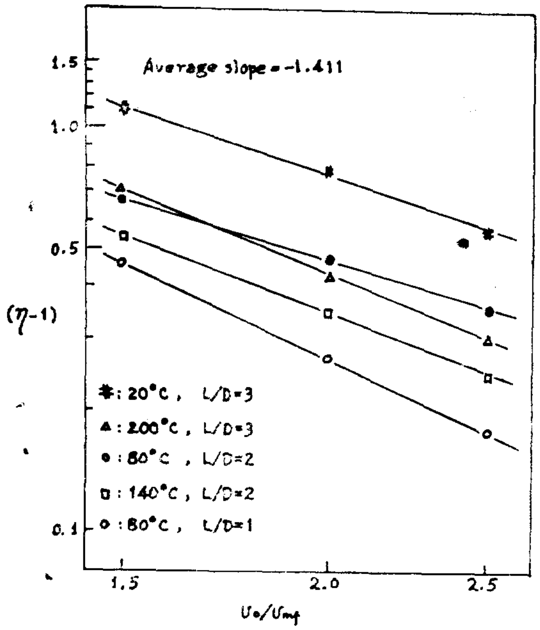

Fig. 6. $(\eta-1)$ vs. Air Flow Rate

slightly with temperature elevation. As shown in *Fig.* 8 the exponent c from the slope was

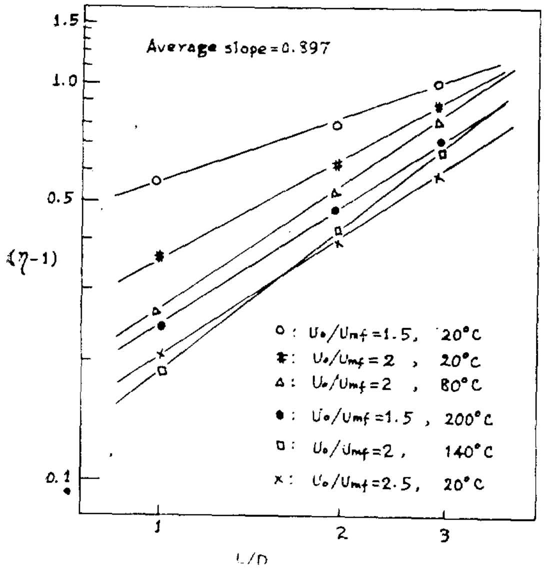

Fig. 7. $(\eta-1)$ vs. Aspect Ratio

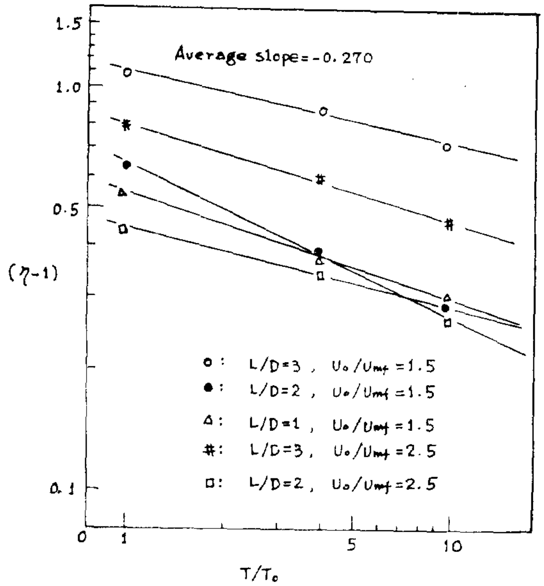

Fig. 8. $(\eta-1)$ vs. Temperature

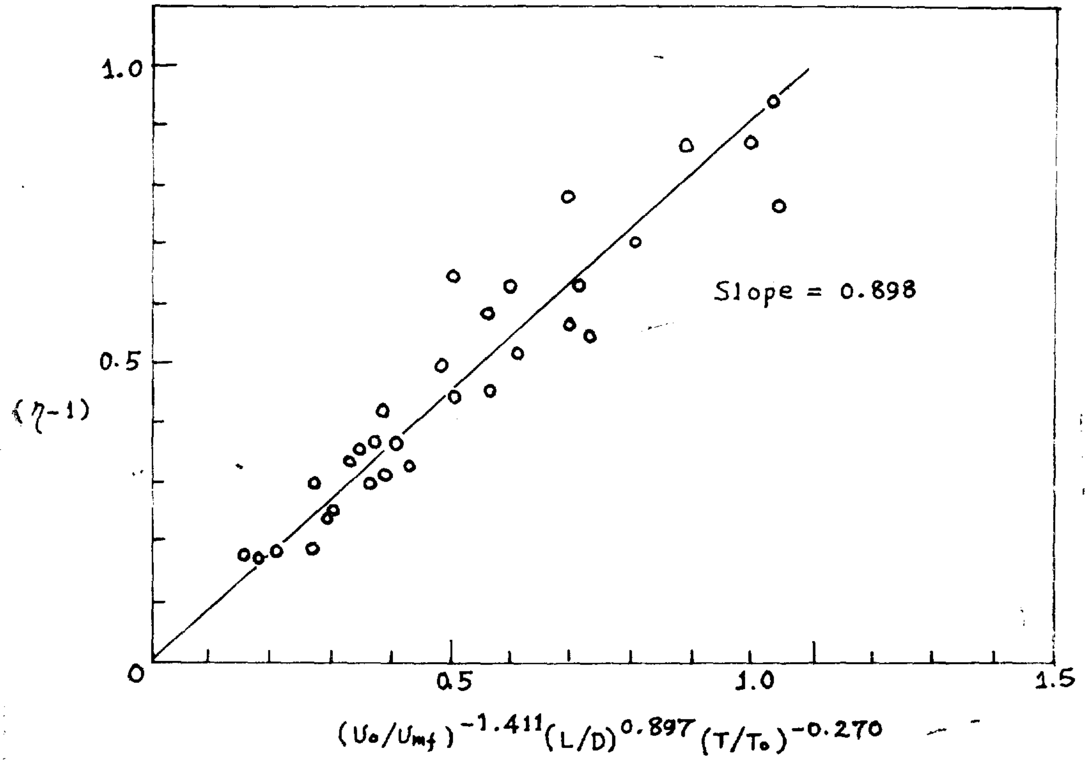

Fig. 9. Correlation of $(\eta-1)$ with Respective Variables

−0.270.

As the results, it followed that the air flow rate and aspect ratio were marked effects on solids mixing, but the temperature elevation was minor.

After substitution of these exponents in Eq (4), the product of the groups within parentheses were calculated and plotted with $(\eta-1)$ as the ordinate (*Fig.* 9). A straight line was obtained, and the average least square values of k was found as 0.898. On substitution, the final correlation became;

$$(\eta-1)=0.898(u_0/u_{mf})^{-1.411}(L/D)^{0.897}(T/T_0)^{-0.270} \quad (5)$$

Ⅴ. Conclusion

The conclusions within the range of these experiments were followings;

1. The onset of fluidization occured earlier than the expected velocity as the temperature rise.
2. Increasing air flow rate increased the backmixing of solids, the bed tended to perfect mixing performance.
3. The more the aspect ratio increased, the more plug flow prevailed.
4. The temperature had minor effect on increasing the solids mixing.

From these observations, the correlation equation between perfect mixing deviation parameter $(\eta-1)$ and respective variables was

$$(\eta-1)=0.898(u_0/u_{mf})^{-1.411}(L/D)^{0.987}(T/T_0)^{-0.270}$$

Ⅵ. Nomenclature

d_p particle diameter, cm
$F(t)$ residence time function
g acceleration of gravity, 980 cm/sec^2
L bed height, cm
Δp pressure drop, g-wt/cm^2
R_{ep} particle Reynolds number, $d_p u_0 \rho_g/\mu$
T temperature, °C
T_0 reference temperature, 20°C
t time, sec
u_0 superficial fluid velocity, cm/sec
u_{mf} minimum fluidization velocity, cm/sec
v volumetric flow rate of solid, cm^3/sec

Greeks

α system phase shift in Eq(1)
ϵ_m void fraction in packed bed
ϵ_{mf} void fraction in a bed at minimum fluidizing condition
ρ_g fluid density, gm/cm^3
ρ_s density of solid, gm/cm^3
ϕ sphericity of a particle
η coefficient of exponent in Eq(1)
θ average residence time
μ viscosity of gas, g/cm-sec

Ⅶ. References

1. E.J. Caurns, J.M. Pransnize, *AIChE. J.*, **6** (1960) 400.
2. P.V. Dankwerts, *Chem. Eng.*, **37**, No. 1 (1953) 1.
3. D. Kunii, O. Levenspiel, "Fluidization Engineering," John Wiley and Sons, Inc., N.Y., 1969.
4. M. Leva, "Fluidization," McGraw-Hill Book Co. Inc., N.Y., 1959.
5. D.R. Morris, K.E. Gubbins, S.B. Watkins, *Trans. Instn. Chem. Engrs.*, **42** (1964) T 323.
6. D. Wolf, W. Resnick, *I & EC Fun.*, **2**, No. 4 (1963) 287.
7. S. Tone, I. Oda, K. Kawamura, and T. Odaka, *J. Chem. Eng. Japan*, **5**, No. 1 (1972) 68.
8. A.W. Loven, *Chem. Eng. Prog.*, **69**, No. 11 (1973) 56.
9. T. Mii, K. Yoshida, D. Kunii, *J. Chem. Eng. Japan*, **6**, No. 1 (1973) 1.
10. D. Kunii, *I & EC Fun.*, **7** (1968) 446.